Published in final edited form as:

Circulation. 2017 November 14; 136(20): 1920–1935. doi:10.1161/CIRCULATIONAHA.117.027589.

Upregulation of HERV-K is Linked to Immunity and Inflammation in Pulmonary Arterial Hypertension

Toshie Saito, MD[1,2,3], **Kazuya Miyagawa, MD, PhD**[1,2,3], **Shih-Yu Chen, MD, PhD**[4,5], **Rasa Tamosiuniene, MD, PhD**[1,2,6], **Lingli Wang, MD**[1,2,3], **Orr Sharpe, MSc**[6], **Erik Samayoa, BS, CLS**[9,10], **Daisuke Harada, PhD**[6], **Jan-Renier A. J. Moonen, MD, PhD**[1,2,3], **Aiqin Cao, PhD**[1,2,3], **Pin-I Chen, PhD**[1,2,3], **Jan K. Hennigs, MD**[1,2,3], **Mingxia Gu, MD, PhD**[1,2,3], **Caiyun G. Li, PhD**[1,2,3], **Ryan D. Leib, PhD**[7], **Dan Li, PhD**[1,2,3], **Christopher M. Adams, PhD**[7], **Patricia A. del Rosario, BSN, RN, PHN**[1,6], **Matthew Bill, BS**[1,6], **Francois Haddad, MD**[2,6], **Jose G. Montoya, MD**[6], **William H. Robinson, MD, PhD**[6], **Wendy J. Fantl, PhD**[4,5,8], **Garry P. Nolan, PhD**[4,5], **Roham T. Zamanian, MD**[1,2,6], **Mark R. Nicolls, MD**[1,2,6], **Charles Y. Chiu, MD, PhD**[9,10], **Maria E. Ariza, PhD**[11], and **Marlene Rabinovitch, MD**[1,2,3]

[1]The Vera Moulton Wall Center for Pulmonary Vascular Disease, Stanford University School of Medicine, Stanford, CA 94305

[2]Cardiovascular Institute, Stanford University School of Medicine, Stanford, CA 94305

[3]Department of Pediatrics, Stanford University School of Medicine, Stanford, CA 94305

[4]Department of Microbiology and Immunology, Stanford University School of Medicine, Stanford, CA 94305

[5]Baxer Laboratory in Stem Cell Biology, Stanford University School of Medicine, Stanford, CA 94305

[6]Department of Medicine, Stanford University School of Medicine, Stanford, CA 94305

[7]Vincent Coates Foundation Mass Spectrometry Laboratory, Stanford University School of Medicine, Stanford, CA 94305

[8]Department of Obstetrics and Gynecology, Stanford University School of Medicine, Stanford, CA 94305

Address for correspondence: Marlene Rabinovitch, MD, Stanford University School of Medicine, CSSR 1215A, 269 Campus Drive, Stanford, CA 94305, Tel: 650 723 8239; FAX: 650 723 6700, marlener@stanford.edu.

Author Contributions

TS and MR designed the experiments, analyzed and interpreted the data and wrote the manuscript. LW, KM and RT helped with the animal experiments. SC, PI-C, JKH, WJF and GPN assisted with CyTOF experiments. JRAJM assisted with confocal microscopic imaging and data analysis. OS, DH and WHR helped with experiments related to immune complex detection. ES and CYC performed unbiased metagenomic next-generation sequencing and computational analysis of the sequence data. MEA generated and provided HERV-K dUTPase, and advised us on related protocols. AC assisted with immunoblots and ELISAs. CGL assisted with optimization of the C1q IP protocol and the initial IP analysis. RDL and CMA performed mass spectrometry to identify target antigens. PA del R, MB and RTZ maintain the Stanford Pulmonary Hypertension Biobank and the PHBI cell inventory, and provided samples and the clinical data for the PAH patients and FH and JGM obtained control samples under the same conditions. MG provided the iPSC and differentiated iPSC-EC, DL helped with immunoblots, MRN critically reviewed the manuscript.

Disclosures

None

[9]Department of Laboratory Medicine and Medicine/Infectious Diseases, University of California, San Francisco, CA 94107

[10]UCSF Viral Diagnostics and Discovery Center, University of California, San Francisco, CA 94107

[11]Department of Cancer Biology and Genetics, The Ohio State University Wexner Medical Center, Columbus, OH, 43210

Abstract

Background—Immune dysregulation has been linked to occlusive vascular remodeling in pulmonary arterial hypertension (PAH) that is hereditary, idiopathic or associated with other conditions. Circulating autoantibodies, lung perivascular lymphoid tissue and elevated cytokines have been related to PAH pathogenesis but without clear understanding of how these abnormalities are initiated, perpetuated and connected in the progression of disease. We therefore set out to identify specific target antigens in PAH lung immune complexes as a starting point toward resolving these issues to better inform future application of immunomodulatory therapies.

Methods—Lung immune complexes were isolated and PAH target antigens were identified by liquid chromatography tandem mass spectrometry (LCMS), confirmed by ELISA, and localized by confocal microscopy. One PAH antigen linked to immunity and inflammation was pursued and a link to PAH pathophysiology was investigated by next generation sequencing, functional studies in cultured monocytes and endothelial cells (EC) and hemodynamic and lung studies in a rat.

Results—SAM domain and HD1 domain-containing protein (SAMHD1), an innate immune factor that suppresses HIV replication was identified and confirmed as highly expressed in immune complexes from 16 hereditary and idiopathic PAH vs. 12 control lungs. Elevated SAMHD1 was localized to endothelial cells (EC), perivascular dendritic cells and macrophages and SAMHD1 antibodies were prevalent in tertiary lymphoid tissue. An unbiased screen using metagenomic sequencing related SAMHD1 to increased expression of human endogenous retrovirus K (HERV-K) in PAH vs. control lungs (n=4 each). HERV-K envelope and deoxyuridine triphosphate nucleotidohydrolase (dUTPase) mRNAs were elevated in PAH vs. control lungs (n=10) and proteins were localized to macrophages. HERV-K dUTPase induced SAMHD1 and pro-inflammatory cytokines (e.g., IL6, IL1β and TNFα) in circulating monocytes and pulmonary arterial (PA) EC, and activated B cells. Vulnerability of PAEC to apoptosis was increased by HERV-K dUTPase in an IL6 independent manner. Furthermore, three weekly injections of HERV-K dUTPase induced hemodynamic and vascular changes of pulmonary hypertension in rats (n=8), and elevated IL6.

Conclusions—Our study reveals that upregulation of the endogenous retrovirus HERV-K could both initiate and sustain activation of the immune system and cause vascular changes associated with PAH.

Keywords

SAM domain and HD1 domain-containing protein (SAMHD1); human endogenous retrovirus K (HERV-K); deoxyuridine triphosphate nucleotidohydrolase (dUTPase); pulmonary arterial hypertension (PAH); tertiary lymphoid tissue

Introduction

Pulmonary arterial hypertension (PAH) is a progressive disorder that may be idiopathic (IPAH), hereditary (HPAH), or associated (APAH) with other conditions that include immune/inflammatory diseases such as scleroderma or HIV infection. In all cases, PAH is characterized by endothelial cell (EC) dysfunction, loss of distal pulmonary arteries (PAs), and obliterative changes in more proximal PAs in association with exuberant expansion of cells that progressively occlude the vessel lumen. These features contribute to an elevation in right ventricular systolic pressure that, despite vasodilator therapy, can lead to right heart failure and the need for a lung transplant. Inflammatory and autoimmune processes are inextricably linked to vascular remodeling in PAH[1]. Circulating autoantibodies[2], lung perivascular tertiary lymphoid tissue[3] and elevated cytokines, including IL6, TNFα, and IL1β[4], have been reported in PAH patients.

The link between immunity and clinical PAH is also evident in experimental animal studies. For example, the athymic rat develops severe pulmonary hypertension attributed to lack of regulatory T cells[5]. Production of pathologic antibodies by bronchus-associated lymphoid tissue is observed in monocrotaline-induced pulmonary hypertension in rats[6]. However, neither in PAH nor in experimental pulmonary hypertension have specific target antigens in lung immune complexes been reported, that could provide mechanistic insight into factors that initiate and perpetuate immune dysregulation and their role in the pathophysiology of PAH.

Materials and Methods

Expanded Materials and Methods are provided in the Online Supplement.

Human samples from PAH patients and controls

All human samples used in this study were de-identified but had been obtained by written informed consent under protocols approved by the Administrative Panel on Human Subjects in Medical Research (IRB) at the various sites described in the Supplement. The demographic and other characteristics of PAH patients and healthy controls used in the various studies are provided in Supplemental Tables 1 and 2.

Lung Tissue—Lung tissues from hereditary and idiopathic PAH patients and control subjects (unused donor lungs) were processed and stored as described previously[7].

Cell isolation and culture—PAH patient and donor control PAEC[8] and PA smooth muscle cells (SMC)[9] were harvested as described previously. In some experiments, we used commercially available PAEC. PAEC were cultured in EC media supplemented with 5% fetal bovine serum (FBS), EC growth supplement and penicillin/streptomycin, and used at passage 3–6. PASMC were cultured in smooth muscle cell media supplemented with 5% FBS, SMC growth supplement and gentamicin/amphotericin-B and used at passage 4–10. Induced pluripotent stem cells derived from fibroblasts and differentiated EC were generated by previously published protocols[8,10].

Peripheral blood mononuclear cells (PBMC)—PBMC were separated by Ficoll-Paque following centrifugation of whole blood at 400 g for 30 min. PBMC ($1X10^7$) were used for further preparation of enriched monocytes. Cells that attached to wells after two hours represented an enriched monocyte preparation. For detection of HERV-K dUTPase in monocytes by qPCR, we used the Pan Monocyte Isolation kit, according to the manufacturer's protocol. PBMC were cultured with RPMI-1640, supplemented with 10% FBS and penicillin/streptomycin.

HERV-K dUTPase protein purification

Recombinant HERV-K dUTPase protein was provided by Dr. Ariza. The herv-k gene encoding the dUTPase was cloned into the pTrcHis Topo TA expression vector and the sequence verified by DNA sequencing analysis, as previously described[11]. The purity of the protein was assessed by SDS-PAGE and capillary-liquid chromatography nanospray tandem mass spectrometry (nano-LC/MSMS) performed at the Ohio State University Mass Spectrometry and Proteomics Facility[11]. High purity dUTPase preparations[11], free of contaminating DNA, RNA, lipopolysaccharide and peptidoglycan, were used.

Treatment of cells with HERV-K dUTPase recombinant protein or lipopolysaccharide (LPS)

PAEC (1×10^6), PBMCs (1×10^6), or enriched monocytes (isolated from 1×10^7 PBMCs as described above) were used. Cells were incubated with 0.1, 1.0, or 10 μg/ml of recombinant HERV-K dUTPase for 24 hr. Culture supernatants were collected for cytokine measurement by ELISA, and cell lysates were used for western immunoblotting. PBMC were analyzed by single mass cytometry (CyTOF). PAEC were also assessed for apoptosis judged by heightened caspase activity during serum withdrawal[8] for 16 hr, when HERV-K dUTPase was added. PASMC were assessed for proliferation (MTT cell proliferation assay) in response to HERV-K dUTPase for 48 hr. In some experiments, IL6 neutralizing antibody vs. isotype control was used to assess whether PAEC apoptosis induced by HERV-K dUTPase was IL6 dependent. In some experiments, monocytes and PAEC were treated with 1 μg/ml LPS for 6 hr and cell lysates were used for qPCR to asses HERV-K dUTPase mRNA.

Immunohistochemistry

Formaldehyde-fixed, paraffin-embedded tissue sections were deparaffinized and permeabilized with 0.2% Triton. Antigen retrieval was done with either citrate buffer pH 6.0 or 1 mM EDTA pH 8.0, depending on the primary antibodies. Sections were immersed in 0.3% hydrogen peroxide, blocked with 5% goat serum and stained with primary antibodies. The following primary antibodies were used: SAMHD1 (1:500), CD3 (1:50), CD19 (1:100), Plasma Cell (1:100), Follicular Dendritic cell (FDC) (1:50), IL6 (1:1000). After incubation with secondary antibodies and amplification with streptavidin-biotin, sections were stained with 3,3-diaminobenzidine (DAB) and counterstained with hematoxylin.

Immunofluorescent staining

Tissue sections were processed as described above, using primary antibodies for SAMHD1 (1:500), VVF (1:1000), CD11c (1:100), CD68 (1:100), CD3 (1:50), HERV-K env (1:1000), HERV-K dUTPase (1:2000, provided by Dr. Ariza), α-Actin (1:400), followed by

fluorescent- conjugated secondary antibodies, Alexa Fluor 488 anti mouse (1:800) or Alexa Fluor 594 anti rabbit antibodies (1:800). Nuclei were stained with DAPI. Images were acquired using a FlouView 1000 or a Leica TCS SP8 confocal microscope.

In situ SAMHD1 antibody production

To localize SAMHD1 antibody producing cells, frozen lung tissues were fixed with acetone blocked with 5% normal goat serum and incubated with GST-tagged SAMHD1 recombinant protein in PBS (20 μg/ml) overnight at 4°C. Sections were washed with PBS and incubated with FITC-conjugated anti GST antibody (1:800) for one hour at RT. Nuclei were stained with DAPI. Images were acquired using a FlouView 1000 confocal microscope.

Immune complex immunoprecipitation and mass spectrometry to identify target antigens

Immune complexes were captured using a Direct IP kit, according to the manufacturer's protocol. The samples were then prepared using filter aided sample preparation (FASP)[12]. Following a buffer exchange, digestion using trypsin was performed on the membrane filter overnight at 37°C, where peptides were spun out, collected and further cleaned on C18 reverse phase material and analyzed by liquid chromatography (LC) and mass spectrometry (MSMS). The raw data were converted to .mgf format and searched by Byonic (Protein Metrics) using typical search conditions and a 1% False Discovery Rate determined using the standard reverse decoy strategy. Byonic output files were further analyzed using custom scripts developed in Matlab to aid in data visualization. We excluded proteins where we did not observe at least 3 peptides in at least one sample. Common contaminants were also excluded. For all other proteins, control and PAH patient data were assessed using significance analysis of microarray (SAM) to determine q values and a false discovery rate (FDR) cutoff of 5%.

Quantification of SAMHD1 specific Immune complexes

Lung tissue (100 mg) was lysed using a dounce homogenizer and 500 μl of lysis buffer (0.025 M Tris-HCl pH 7.5, 0.15 M NaCl, 1 mM EDTA, 0.5% NP40, 5% glycerol) with proteinase/phosphatase inhibitors. After centrifugation at 20,000 g for 20 min at 4°C, total protein concentration of the supernatant was measured and diluted in PBS to 1 μg/μl total protein. ELISA plates were coated with 0.02 mg/mL SAMHD1 antibody in PBS overnight at 4°C. The plates were blocked with 5% BSA in PBS for one hour. Lung lysate was applied and incubated for two hours. HRP-conjugated species-specific anti human IgG added to the plates, and incubated for 1 hr at room temperature. Tetramethylbenzidine substrate was added for 15 min, then the reaction was stopped with 2 N sulfuric acid, and OD values were determined at 450 nm.

Western immunoblotting

Lung lysates (50 mg) were prepared by homogenization with 500 μl of modified RIPA buffer (50 mM Tris-HCl pH 7.4, 150 mM NaCl, 1 mM EDTA, 1% Triton X-100, 0.1% SDS, 1% Sodium deoxycholate, 1 mM PMSF) containing protease and phosphatase inhibitors. After centrifugation at 20,000 g for 20 min at 4°C, the supernatant was collected. Protein concentration was determined by BCA. Equal amounts of protein were loaded on a precast

NuPage 4–12% Bis-Tris gel and subjected to electrophoresis under reducing conditions and electrotransferred onto polyvinylidene difluoride (PVDF) membranes. After blocking with 5% milk in 0.5% Tween-PBS, membranes were incubated with primary antibodies against SAMHD1 (1:500), pSTAT3 (1:1000), STAT3 (1:1000), β-Actin (1:10000), α-Tubulin (1:2000). Anti mouse IgG secondary antibody (1:5000) was used. After incubation with HRP-conjugated secondary antibodies, signals were visualized with ECL or ECL prime.

Enzyme-linked immunosorbent assay (ELISA)

Cytokine levels in human enriched monocytes, human PAEC and rat lung lysates were measured using the Quantikine ELISA kit for human TNFα, IL1β and IL6 and rat IL6, according to the manufacturer's protocol.

Quantitative (q)PCR

Total RNA was extracted and purified from lung tissue or cells using spin column based kits. RT-PCR was performed according to the manufacture's protocol. qPCR was performed with a 7900HT Sequence Detection System or a CFX384 Real Time System. Primers used: TaqMan Gene Expression Assays, (β-actin (Hs01060665_g1), HERV-K(II) env (PN4441114, custom probe, Applied Biosystems) and Syber Green assays, HERV-K dUTPase (Forward, 5′-AAATGGGCAACCATTGTCGGGAAACGAGC-3′; Reverse, 5′-TAGTACATAAATCTACTGCTGCACTGC-3), β-actin (Forward, 5′-CATGCCATCCTGCGTCTGGA-3′; Reverse, 5′-CCGTGGCCATCTCTTGCTCG).

Unbiased pan-viral metagenomic next-generation sequencing

Samples were sequenced on an Illumina MiSeq instrument using 300/200 base pair (bp) paired-end sequencing. Approximately 18.3 million sequencing reads were analyzed using a modified version of SURPI (Sequence-Based Ultra-Rapid Pathogen Identification)[13], a computational pipeline for detection of microbes, including viruses, from next-generation sequencing data. Viral reads were identified as HERVs using a stringent edit distance requirement of 0 (no mismatches) across 75 bp of sequence. HERV reads were also taxonomically classified to the appropriate rank (family, genus, species, or subspecies/strain) by use of an in-house developed classification algorithm using the SNAP nucleotide aligner (v0.15)[13]. Heat maps were generated using matrix2png[14].

CyTOF (single cell mass cytometry)

PBMC were stained with metal-conjugated antibodies and analyzed with a mass cytometer. $1X10^6$ cells were used for each sample. Concatenated data were normalized using NormalizerR2013b and de-barcoded using the Matlab DebarcoderR2013b. Gating was performed in http://nolanlab.cytobank.org[15]. The data were transformed to arcsinh values by taking the inverse hyperbolic sine of the raw data. The arcsinh ratio is the difference between the median arcsinh values of the two samples. Data from PAH and controls are shown as arcsinh ratio normalized for assay control. Data for HERV-K dUTPase reflect treated over untreated (control) PBMCs (Stanford Blood Bank). Information about metal-conjugated antibodies is provided in the Online Supplement.

Rat model for the induction of pulmonary hypertension by HERV-K dUTPase

The Animal Care Committee at Stanford University approved all experimental protocols used in this study, following the published guidelines of the National Institutes of Health and the American Physiological Society. Adult male Sprague-Dawley rats (7 wks, 180–200 g) were randomly assigned to a control or treatment group. Rats were either untreated or given a single subcutaneous dose of SU5416 (20 mg/kg body weight)[5] one day prior to the first of three weekly intravenous injections of HERV-K dUTPase (0.2 mg/kg body weight) in saline. Rats in the control group were treated with saline vehicle. Twenty-one days after the first HERV-K dUTPase injection, cardiac function, right ventricular systolic pressure and right ventricular hypertrophy were assessed as previously described[7]. Isoflurane anesthesia (1.5%, 1 liter/min oxygen) was used during these procedures. Lung tissues were assessed by histology and ELISA. For histology, staining methods are described above. Quantification of muscularization and arterial number relative to alveoli was conducted in a blinded manner, and details are provided in the Online Supplement. Images were acquired using a Leica DMLB microscope (Leica, Buffalo Grove. For the measurement of IL6 by ELISA, 20 μg of lung tissue was homogenized. After centrifugation, the total protein concentration of the supernatant was measured and prepared in PBS at a concentration of 0.5 μg/μL.

Statistical Analysis

Data were analyzed using Prism 6.0 (GraphPad Software, La Jolla, CA). Statistical significance was determined by one-way ANOVA followed by Dunnett's test or Tukey's test of multiple comparisons when more than two groups were being compared. When only two groups were compared, we used Student's t-test. For some experiments, as indicated in the figure legends, we applied the Welch or Mann Whitney test depending on the data distribution, i.e., when the distribution was not normal we used the Mann-Whitney and when the variance was unequal by F-test, we used the Welch. A P-value of <0.05 was considered significant. Data are shown as mean ±SEM or median with interquartile range depending on the test applied. For target identification of immune complexes by mass spectrometry, significance analysis of microarray (SAM) was applied with false discovery rate (FDR) cutoff of 5%[16]. For signaling data by CyTOF, Bonferroni-adjusted P-value ($P=7.14X10^{-3}$) was applied to signaling response with arcsinh ratio $>|0.2|$[17].

Accession Numbers

Next-generation sequencing data with human sequences removed, using BLASTn to the human genome at a low-stringency cutoff of 10^{-5} have been publicly deposited in the NIH Sequence Read Archive (SRA accession number SRP056561).

Results

SAMHD1 is a target antigen in immune complexes in PAH lungs

We obtained lung tissues from unused donor lungs as controls and from patients with idiopathic or hereditary PAH (designated as PAH in the text) from the Pulmonary Hypertension Breakthrough Initiative (PHBI) Network. The characteristics of PAH patients and controls are provided in Supplementary Tables 1 and 2. To determine whether the target

antigens of lung immune complexes differed in PAH vs. control lungs, three PAH and three control lung samples were captured by complement 1q (C1q) immunoprecipitation, eluted, subjected to filter-aided sample preparation (FASP)[12] and analyzed by liquid chromatography tandem mass spectrometry (LC/MSMS). The top samples ranked based upon q value and a FDR<5%[16] are shown in Figure 1A. Of particular interest was SAM domain and HD1 domain-containing protein (SAMHD1) that was highly represented in PAH samples vs. controls. SAMHD1 has been related to autoimmunity[18] and HIV infection[19], conditions associated with PAH.

We therefore expanded our analysis to a larger cohort of 16 PAH and 12 control lungs and confirmed a significant increase in the level of SAMHD1 immune complexes in the PAH lungs (Figure 1B). We next investigated the source of the SAMHD1 antibodies in PAH lungs. Tertiary lymphoid tissue which is associated with chronic inflammation and autoimmune diseases[20] is particularly prominent in PAH lungs[3]. We confirmed these findings (Figure 1C, D), and investigated whether the tertiary lymph nodes are the source of SAMHD1 antibodies. Following the addition of recombinant GST-tagged SAMHD1 protein to lung tissue sections and incubation of the tissue with an anti-GST-FITC-conjugated antibody, we observed SAMHD1 immunoreactive foci in the perivascular tertiary lymphoid tissue (Figure 1E), suggesting that these structures are the likely source of SAMHD1 antibody production.

Elevated SAMHD1 in PAH lung cells and in circulating classical dendritic cells

In PAH lungs, SAMHD1 immune complexes were associated with heightened expression of SAMHD1 in lung lysates as assessed by western immunoblot (Figure 2A). The site of increased expression of SAMHD1 in PAH lungs was localized to the perivascular region as well to the vessel wall, whereas in control lungs, SAMHD1 positive cells were scattered in the lung parenchyma and excluded from the arterial walls (Figure 2B). To determine the cellular localization of SAMHD1, we performed confocal microscopy analysis in tissue sections double-immunolabeled with antibodies to SAMHD1 and either von Willebrand factor (vWF) to detect pulmonary artery endothelial cells (PAEC), CD68 as a marker of macrophages, CD11c for dendritic cells and CD3 for T cells (Figure 2C). Almost all SAMHD1 positive cells in the perivascular/vascular region co-expressed markers for macrophages, dendritic cells and endothelial cells, but not for T cells. The heightened expression of SAMHD1 in PAH was also confirmed in circulating classical dendritic cells (cDC) (Figure 2D, with details of gating in Supplemental Figure 1A) assessed as part of a larger analysis applying single cell mass cytometry (CyTOF)[15] to peripheral blood mononuclear cells (PBMC).

Human endogenous retrovirus-K (HERV-K) and its products HERV-K envelope and dUTPase are increased in IPAH

We next investigated whether SAMHD1 could be induced as an innate immune response[21] to an exogenous virus. In addition to HIV[22], the Kaposi sarcoma virus (Human herpesvirus 8)[23] and hepatitis C virus[24] have been associated with PAH in some series, but not others[25]. We therefore subjected flash frozen lung tissue from four PAH patients and four controls to a blinded unbiased metagenomic viral screen, using the Illumina MiSeq next-generation

sequencing platform and the SURPI computational pipeline, to identify viral sequences[13, 26]. Consistent with a previous series[25], we did not detect viruses that were previously implicated in PAH in our lung samples, nor did we detect other known exogenous viruses. However, we observed a significant increase in the percentage of human endogenous retroviral sequences in PAH lung samples relative to controls, in particular HERV-K[27] family members (Figure 3A).

The HERV-K family comprises less than 1% of the HERV sequences found in the human genome and are transcriptionally active. Although in theory an infectious virus could be produced, mutations interrupting the virus open reading frames (ORFs) lead to degenerate sequences that makes it highly unlikely. However, expression of HERV-K encoded proteins have been shown to induce viral restriction pathways in early embryonic cells[28]. Furthermore, increased expression of HERVs proteins, including the envelope protein and the dUTPase, have been linked to cancer[29], multiple sclerosis[30], systemic lupus erythematosus[31] and rheumatoid arthritis[32]. Also, the psoriasis susceptibility 1 (*PSORS1)* locus, identified as the strongest genetic determinant of psoriasis, harbors a HERV-K that encodes for a dUTPase[33, 34]. We confirmed a significant induction in the HERV-K(II) envelope and HERV-K dUTPase mRNA in PAH lungs vs. controls (Figure 3B). Confocal microscopy demonstrated that an increase in HERV-K envelope and dUTPase proteins were primarily present in perivascular $CD68^+$ macrophages, that are abundant in PAH lungs (Figure 3C). We further confirmed that circulating monocytes from PAH patients exhibit higher mRNA levels of HERV-K dUTPase relative to control cells (Figure 3D).

HERV-K dUTPase increases SAMHD1 and cytokines in enriched monocytes and in PAEC, and activates B cells

The HERV-K dUTPase induces the secretion of Th1 and Th17 cytokines involved in the formation of psoriatic plaques, independent of its enzymatic activity[11], thus associating HERV-K to the pathology of psoriasis. Having confirmed the higher HERV-K dUTPase in PAH lung macrophages and circulating monocytes (Figure 3B–D), we determined whether recombinant HERV-K dUTPase could induce SAMHD1. Indeed, HERV-K dTUPase induces SAMHD1 both in enriched monocytes and in PAEC (Figure 4A, B). Furthermore, HERV-K dUTPase induces in enriched monocytes a profile of cytokines that are implicated in PAH, namely TNFα, IL1β and IL6[4], (Figure 4C). We also observed induction of IL6 by HERV-K dUTPase in PAEC (Figure 4D). Moreover, we found that HERV-K dUTPase can activate B cells, as determined by CD69 expression (Figure 4E; details of gating in Supplemental Figure 1B), as well as STAT3 signaling (Figure 4F), consistent with a response related to the production of immunoglobulins[35]. Taken together, our observations related to expansion of HERV-K and the sequelae of its dUTPase are consistent with chronic induction of inflammation and altered immunity observed in PAH.

HERV-K dUTPase induces apoptosis in PAEC

Since increased vulnerability to apoptosis is a feature of PAH PAEC[8], we assessed the functional impact of HERV-K dUTPase on PAEC survival following serum withdrawal by the Caspase 3/7 assay. HERV-K dUTPase enhanced PAEC apoptosis following serum withdrawal (Figure 5A), as did co-culture with HERV-K dUTPase-treated monocytes

(Supplemental Figure 2A). To determine whether the enhanced PAEC apoptosis was related to induction of IL6, we pretreated the cells with an IL6 neutralizing antibody vs. an isotype control (Figure 5B). We verified the suppression of PBMC pSTAT3 in response to IL6 by the neutralizing antibody as a measure of its efficacy, (Supplemental Figure 2B) but could not detect a significant impact of blocking IL6 on HERV-K mediated enhanced PAEC apoptosis (Figure 5B). There was no effect of HERV-K dUTPase on PASMC, proliferation assessed by MTT assay at 48 hours (Supplemental Figure 2C).

HERV-K dUTPase is induced by inflammatory stimuli

As circulating PAH monocytes have increased HERV-K dUTPase expression and are exposed to a high cytokine milieu[4], we determined whether inflammatory stimuli that can be genotoxic[36] could upregulate HERV-K dUTPase mRNA. Indeed, lipopolysaccharide (LPS) treatment increased HERV-K dUTPase in monocytes (Figure 5C) but not in PAEC (Supplemental Figure 2D). To determine whether induction of HERV-K could be cell specific, we also evaluated HERV-K dUTPase mRNA levels in iPSC since reprogramming of fibroblasts is known to induce an inflammatory response[37]. In fact, it was observed in a previous study that HERVs are transiently hyper-activated during reprogramming toward iPSC and play an important role in this process[38]. However, once reprograming is complete and cells acquire full pluripotency, HERV activity decreases[38]. iPSC from PAH patients vs. controls demonstrate higher HERV-K dUTPase mRNA levels (Figure 5D) suggesting that some intrinsic factor induces higher levels of HERV-K dUTPase mRNA in PAH cells responding to an environmental or genotoxic stress. Interestingly, the differentiated EC did not show up-regulation of HERV-K dUTPase mRNA (Supplemental Figure 2E). Nor was there an increase in HERV-K dUTPase mRNA in cultured PAH vs. Control PAEC (Supplemental Figure 2F) or PASMC (Supplemental Figure 2G). This suggests that propensity to HERV-K upregulation in response to an environmental stress is cell-specific.

HERV-K dUTPase causes pulmonary hypertension in a rat model

To further substantiate a cause and effect relationship between HERV-K amplification, dUTPase production and pulmonary hypertension, we delivered HERV-K dUTPase (0.2 mg/kg) by intravenous injection, once a week for three weeks, to adult male Sprague Dawley (SD) rats. Rats treated with HERV-K dUTPase exhibited decreased pulmonary artery acceleration time (PAAT), increased right ventricular systolic blood pressure (RVSP) and right ventricular hypertrophy (RVH) compared to saline-injected rats (Figure 6A–C). These features were associated with adverse remodeling of the pulmonary circulation judged by increased muscularization of distal PAs (Figure 6D). Cardiac output, ejection fraction and the number of vessels per 100 alveoli in the lung were not affected by HERV-K dUTPase treatment (Supplemental Figure 3). We further assessed the impact of HERV-K dUTPase in combination with the VEGF receptor 2 blocker SU5416 (Sugen) on pulmonary hypertension in rats[5]. We observed that three weekly injection of HERV-K dUTPase with Sugen pretreatment resulted in increased pulmonary hypertension as judged by a reduced pulmonary artery acceleration time (PAAT), increased right ventricular systolic blood pressure (RVSP) and right ventricular hypertrophy (RVH), muscularization of peripheral arteries when compared to SU5416 only injected rats (Figure 6A–D).

HERV-K dUTPase induced IL6 in enriched monocytes and in PAEC (Figure 4C, D). Heightened circulating levels of IL6 are observed in patients with PAH[4] and a transgenic mouse with IL6 overexpression develops spontaneous pulmonary hypertension[39]. Indeed, rats injected intravenously with HERV-K dUTPase, with or without pretreatment with SU5416 exhibited increased IL6 by ELISA in lung tissue harvested from the rats at the end of the experimental period (Figure 6E), that was localized to PAEC and perivascular inflammatory cells (Figure 6F).

Discussion

Several emerging therapies for PAH target the abnormal immune and inflammatory response linked to the pathology of PAH[1]. However, the key features that sustain immune dysregulation have not been elucidated. The identification of SAMHD1 led to the discovery of upregulation of the sequences encoding the retrovirus HERV-K and its product, dUTPase, in PAH lungs, circulating monocytes and iPSCs. Combined with the finding that injection of HERV-K dUTPase induced pulmonary hypertension in a rat model, we propose that activation of endogenous retrovirus sequences and expression of their gene products may underlie the chronic inflammatory and altered immune state associated with progressive vascular remodeling in PAH (see schema in Figure 7).

Diseases associated with HERV-K are complex diseases that probably represent the interaction of several factors including genetic susceptibility as well as the microenvironment or location of cellular injury, for example neuronal injury may lead to expansion of HERVs in association with multiple sclerosis[30]. Morphea, also known as localized scleroderma is linked to local upregulation of HERVs in skin[40].

HIV is linked to PAH[22] and the potential relationship between HIV as an activator of HERV's is well documented in previous studies. For example, HIV-1 Tat protein induces HERV-K mRNA and HERV-K mRNA in PBMC from HIV-1-infected patients is increased compared to HIV negative controls[41].

While the genes associated with HERV-K are present in all cell types, they may differ in the expression levels due perhaps to epigenetic features and mechanisms of RNA translation that can be regulated by metabolism and by the cellular microenvironment[42]. In tissues from PAH patients, high levels of HERV-K expression in perivascular CD68+ cells may be sufficient to induce paracrine effects on vascular cells and B cells that promote PAH pathology.

Cells exposed to genotoxic agents that include oxidant stress, gamma irradiation, viruses and cytokines show increased expression of endogenous retroviruses[43]. Genomic instability is a feature of PAH[44], attributed to impaired DNA repair in response to a genotoxic stress[45], that could lead to unresolved cell-specific expansion of HERV-K and sustained immune dysregulation. LPS upregulated HERV-K in monocytes and it is an environmental stress that can be genotoxic[36]. Reprogramming in induced pluripotent stem cells, that is known to mediate an immune response, was linked to a PAH related increase in HERV-K. The

mechanism causing the propensity for upregulation of HERV-K in certain PAH cell types would be interesting to investigate in future studies.

The expansion of HERV-K mRNA sequences has been related both to NFκB-mediated transcription and to a decrease in the methyl transferase SETDB1[46]. Enhanced HERV-K mRNA translation has also been described under conditions of cellular stress and attributed to an increase in Staufin 1 (Stau 1). Stau1 is a binding partner for HERV-K capsid protein and when Stau1 is overexpressed there is rapid translation of HERV-K sequences. Stau1 prevents EIF2α mediated stress granule formation, thereby facilitating mRNA translation under conditions of cellular stress[47]. This aberrant feature, impaired stress granule formation and heightened mRNA translation in response to inflammatory stress, was described by our group in PAEC with reduced BMPR2[7], a key feature of PAH, owing to impaired phosphorylation of the elongation factor EIF2α. It is therefore interesting that a mutation in a kinase that phosphorylates EIF2α, EIF2K4A (also known as GCN2), has been described in families with pulmonary veno-occlusive disease[48] and has also been identified in some patients with hereditary PAH (Graf et al., American Journal of Respiratory and Critical Care Medicine, ATS abstracts, 2016).

We demonstrated that HERV-K dUTPase activates monocytes, leading to elevated production of cytokines (TNFα, IL6 and IL1β), and SAMHD1. HERV-K dUTPase activates B cells, in a manner that could be responsible for local production of SAMHD1 antibodies in tertiary lymphoid tissue in PAH lungs. While identification of the SAMHD1 antibodies led us to the identification of HERV-K, immune complexes and activation of complement have also been linked to pulmonary hypertension[49]. However, we do not know whether there is heightened immunogenicity of SAMHD1 immune complexes.

HERV-K dUTPase inoculation is sufficient to cause PH in rats. Our model suggests a sustained effect of the dUTPase, as IL6 was still elevated in the lung and localized to inflammatory and ECs a week after the third injection. While sustained elevation of IL6 levels could be responsible for pulmonary hypertension, as was seen in the transgenic IL6 overexpressing mouse[39], other factors independent of IL6 such as those that control EC susceptibility to apoptosis can also contribute to the pathology. It would be of interest to address the nature of endogenous retrovirus elements that are expressed in rodent models of pulmonary hypertension but these elements are very numerous and a dUTPase with homology to HERV-K has not been identified[50].

Due to the complexity of human disease, it is difficult to prove a cause and effect relationship rather than an association between viral infection[23, 24] or endogenous retroviruses and PAH. More comprehensive analysis of the mechanism of upregulation of retroviral sequences in PAH could lead to strategies to assess the impact of blocking the production of these elements.

In summary, our findings show how upregulation of HERV-K could induce and perpetuate chronic immune dysfunction and inflammation and endothelial dysfunction leading to adverse remodeling related to PAH.

Supplementary Material

Refer to Web version on PubMed Central for supplementary material.

Acknowledgments

We greatly appreciate the editorial and technical assistance of Dr. Michal Bental Roof in preparing both the manuscript and figures, and the administrative help of Ms. Michelle Fox.

Sources of Funding

Supported by NIH/National Heart Lung and Blood Institute grants N01 HV00242 (MR, WHR, MRN, RTZ), R01 HL08HERV62 (MRN), R24 HL123767 (MR), NIH/National Institute of Allergy and Infectious Diseases grant R01 A1084898 (MEA), Cardiovascular Medical Research and Education Fund (CMREF) Grant UL1 RR024986 (MR) and an endowed Dwight and Vera Dunlevie Chair in Pediatric Cardiology (MR). Mass spectrometry resources were purchased with the assistance of NIH/National Center for Research Resources award S10RR027425. KM was supported by fellowships from Japan Heart Foundation/Bayer Yakuhin Research Grant Abroad and The Uehara Memorial Foundation. JKH was supported by grant He 6855/1-1 from Deutsche Forschungsgemeinschaft, and JRAJM is supported by the Netherlands Heart Foundation Grant 2013T116. ES and CYC were partially supported by NIH/NHLBI grant R01 HL105704 (CYC) and research funding from Abbott Laboratories, Inc.

References

1. Rabinovitch M, Guignabert C, Humbert M, Nicolls MR. Inflammation and immunity in the pathogenesis of pulmonary arterial hypertension. Circ Res. 2014; 115:165–175. [PubMed: 24951765]
2. Dib H, Tamby MC, Bussone G, Regent A, Berezne A, Lafine C, Broussard C, Simonneau G, Guillevin L, Witko-Sarsat V, Humbert M, Mouthon L. Targets of anti-endothelial cell antibodies in pulmonary hypertension and scleroderma. Eur Respir J. 2012; 39:1405–1414. [PubMed: 22005913]
3. Perros F, Dorfmuller P, Montani D, Hammad H, Waelput W, Girerd B, Raymond N, Mercier O, Mussot S, Cohen-Kaminsky S, Humbert M, Lambrecht BN. Pulmonary lymphoid neogenesis in idiopathic pulmonary arterial hypertension. Am J Respir Crit Care Med. 2012; 185:311–321. [PubMed: 22108206]
4. Soon E, Holmes AM, Treacy CM, Doughty NJ, Southgate L, Machado RD, Trembath RC, Jennings S, Barker L, Nicklin P, Walker C, Budd DC, Pepke-Zaba J, Morrell NW. Elevated levels of inflammatory cytokines predict survival in idiopathic and familial pulmonary arterial hypertension. Circulation. 2010; 122:920–927. [PubMed: 20713898]
5. Tamosiuniene R, Tian W, Dhillon G, Wang L, Sung YK, Gera L, Patterson AJ, Agrawal R, Rabinovitch M, Ambler K, Long CS, Voelkel NF, Nicolls MR. Regulatory T cells limit vascular endothelial injury and prevent pulmonary hypertension. Circ Res. 2011; 109:867–879. [PubMed: 21868697]
6. Colvin KL, Cripe PJ, Ivy DD, Stenmark KR, Yeager ME. Bronchus-associated lymphoid tissue in pulmonary hypertension produces pathologic autoantibodies. Am J Respir Crit Care Med. 2013; 188:1126–1136. [PubMed: 24093638]
7. Sawada H, Saito T, Nickel NP, Alastalo TP, Glotzbach JP, Chan R, Haghighat L, Fuchs G, Januszyk M, Cao A, Lai YJ, de Perez VJ, Kim YM, Wang L, Chen PI, Spiekerkoetter E, Mitani Y, Gurtner GC, Sarnow P, Rabinovitch M. Reduced BMPR2 expression induces GM-CSF translation and macrophage recruitment in humans and mice to exacerbate pulmonary hypertension. J Exp Med. 2014; 211:263–280. [PubMed: 24446489]
8. Sa S, Gu M, Chappell J, Shao NY, Ameen M, Elliott KA, Li D, Grubert F, Li CG, Taylor S, Cao A, Ma Y, Fong R, Nguyen L, Wu JC, Snyder MP, Rabinovitch M. Induced pluripotent stem cell model of pulmonary arterial hypertension reveals novel gene expression and patient specificity. Am J Respir Crit Care Med. 2017; 195:930–941. [PubMed: 27779452]
9. Tojais NF, Cao A, Lai YJ, Wang L, Chen PI, Alcazar MAA, de Jesus Perez VA, Hopper RK, Rhodes CJ, Bill MA, Sakai LY, Rabinovitch M. Codependence of bone morphogenetic protein receptor 2

and transforming growth factor-beta in elastic fiber assembly and its perturbation in pulmonary arterial hypertension. Arterioscler Thromb Vasc Biol. 2017; 37:1559–1569. [PubMed: 28619995]

10. Gu M, Shao NY, Sa S, Li D, Termglinchan V, Ameen M, Karakikes I, Sosa G, Grubert F, Lee J, Cao A, Taylor S, Ma Y, Zhao Z, Chappell J, Hamid R, Austin ED, Gold JD, Wu JC, Snyder MP, Rabinovitch M. Patient-specific iPSC-derived endothelial cells uncover pathways that protect against pulmonary hypertension in BMPR2 mutation carriers. Cell Stem Cell. 2017; 20:490–504. e495. [PubMed: 28017794]
11. Ariza ME, Williams MV. A human endogenous retrovirus K dUTPase triggers a TH1, TH17 cytokine response: Does it have a role in psoriasis? J Invest Dermatol. 2011; 131:2419–2427. [PubMed: 21776007]
12. Wisniewski JR, Zougman A, Nagaraj N, Mann M. Universal sample preparation method for proteome analysis. Nat Methods. 2009; 6:359–362. [PubMed: 19377485]
13. Naccache SN, Federman S, Veeraraghavan N, Zaharia M, Lee D, Samayoa E, Bouquet J, Greninger AL, Luk KC, Enge B, Wadford DA, Messenger SL, Genrich GL, Pellegrino K, Grard G, Leroy E, Schneider BS, Fair JN, Martinez MA, Isa P, Crump JA, DeRisi JL, Sittler T, Hackett J Jr, Miller S, Chiu CY. A cloud-compatible bioinformatics pipeline for ultrarapid pathogen identification from next-generation sequencing of clinical samples. Genome Res. 2014; 24:1180–1192. [PubMed: 24899342]
14. Pavlidis P, Noble WS. Matrix2png: A utility for visualizing matrix data. Bioinformatics. 2003; 19:295–296. [PubMed: 12538257]
15. Bendall SC, Simonds EF, Qiu P, Amirel AD, Krutzik PO, Finck R, Bruggner RV, Melamed R, Trejo A, Ornatsky OI, Balderas RS, Plevritis SK, Sachs K, Pe'er D, Tanner SD, Nolan GP. Single-cell mass cytometry of differential immune and drug responses across a human hematopoietic continuum. Science. 2011; 332:687–696. [PubMed: 21551058]
16. Roxas BA, Li Q. Significance analysis of microarray for relative quantitation of LC/MS data in proteomics. BMC Bioinformatics. 2008; 9:187. [PubMed: 18402702]
17. Gaudilliere B, Fragiadakis GK, Bruggner RV, Nicolau M, Finck R, Tingle M, Silva J, Ganio EA, Yeh CG, Maloney WJ, Huddleston JI, Goodman SB, Davis MM, Bendall SC, Fantl WJ, Angst MS, Nolan GP. Clinical recovery from surgery correlates with single-cell immune signatures. Sci Transl Med. 2014; 6:255ra131.
18. Kretschmer S, Wolf C, Konig N, Staroske W, Guck J, Hausler M, Luksch H, Nguyen LA, Kim B, Alexopoulou D, Dahl A, Rapp A, Cardoso MC, Shevchenko A, Lee-Kirsch MA. SAMHD1 prevents autoimmunity by maintaining genome stability. Ann Rheum Dis. 2015; 74:e17. [PubMed: 24445253]
19. Goldstone DC, Ennis-Adeniran V, Hedden JJ, Groom HC, Rice GI, Christodoulou E, Walker PA, Kelly G, Haire LF, Yap MW, de Carvalho LP, Stoye JP, Crow YJ, Taylor IA, Webb M. HIV-1 restriction factor SAMHD1 is a deoxynucleoside triphosphate triphosphohydrolase. Nature. 2011; 480:379–382. [PubMed: 22056990]
20. Aloisi F, Pujol-Borrell R. Lymphoid neogenesis in chronic inflammatory diseases. Nat Rev Immunol. 2006; 6:205–217. [PubMed: 16498451]
21. Sze A, Olagnier D, Lin R, van Grevenynghe J, Hiscott J. SAMHD1 host restriction factor: A link with innate immune sensing of retrovirus infection. J Mol Biol. 2013; 425:4981–4994. [PubMed: 24161438]
22. Flores SC, Almodovar S. Human immunodeficiency virus, herpes virus infections, and pulmonary vascular disease. Pulm Circ. 2013; 3:165–170. [PubMed: 23662195]
23. Cool CD, Rai PR, Yeager ME, Hernandez-Saavedra D, Serls AE, Bull TM, Geraci MW, Brown KK, Routes JM, Tuder RM, Voelkel NF. Expression of human herpesvirus 8 in primary pulmonary hypertension. N Engl J Med. 2003; 349:1113–1122. [PubMed: 13679525]
24. Demir C, Demir M. Effect of hepatitis C virus infection on the right ventricular functions, pulmonary arterypressure and pulmonary vascular resistance. Int J Clin Exp Med. 2014; 7:2314–2318. [PubMed: 25232427]
25. Valmary S, Dorfmuller P, Montani D, Humbert M, Brousset P, Degano B. Human gamma-herpesviruses Epstein-Barr virus and human herpesvirus-8 are not detected in the lungs of patients with severe pulmonary arterial hypertension. Chest. 2011; 139:1310–1316. [PubMed: 21051388]

26. Chiu CY. Viral pathogen discovery. Curr Opin Microbiol. 2013; 16:468–478. [PubMed: 23725672]
27. Hohn O, Hanke K, Bannert N. HERV-K(HML-2), the best preserved family of HERVs: Endogenization, expression, and implications in health and disease. Front Oncol. 2013; 3:246. [PubMed: 24066280]
28. Grow EJ, Flynn RA, Chavez SL, Bayless NL, Wossidlo M, Wesche DJ, Martin L, Ware CB, Blish CA, Chang HY, Pera RA, Wysocka J. Intrinsic retroviral reactivation in human preimplantation embryos and pluripotent cells. Nature. 2015; 522:221–225. [PubMed: 25896322]
29. Johanning GL, Malouf GG, Zheng X, Esteva FJ, Weinstein JN, Wang-Johanning F, Su X. Expression of human endogenous retrovirus-K is strongly associated with the basal-like breast cancer phenotype. Sci Rep. 2017; 7:41960. [PubMed: 28165048]
30. Perron H, Bernard C, Bertrand JB, Lang AB, Popa I, Sanhadji K, Portoukalian J. Endogenous retroviral genes, herpesviruses and gender in multiple sclerosis. J Neurol Sci. 2009; 286:65–72. [PubMed: 19447411]
31. Pullmann R Jr, Bonilla E, Phillips PE, Middleton FA, Perl A. Haplotypes of the HRES-1 endogenous retrovirus are associated with development and disease manifestations of systemic lupus erythematosus. Arthritis Rheum. 2008; 58:532–540. [PubMed: 18240231]
32. Freimanis G, Hooley P, Ejtehadi HD, Ali HA, Veitch A, Rylance PB, Alawi A, Axford J, Nevill A, Murray PG, Nelson PN. A role for human endogenous retrovirus-K (HML-2) in rheumatoid arthritis: Investigating mechanisms of pathogenesis. Clin Exp Immunol. 2010; 160:340–347. [PubMed: 20345981]
33. Foerster J, Nolte I, Junge J, Bruinenberg M, Schweiger S, Spaar K, van der Steege G, Ehlert C, Mulder M, Kalscheuer V, Blumenthal-Barby E, Winter J, Seeman P, Stander M, Sterry W, Te Meerman G. Haplotype sharing analysis identifies a retroviral dUTPase as candidate susceptibility gene for psoriasis. J Invest Dermatol. 2005; 124:99–102. [PubMed: 15654959]
34. Lai OY, Chen H, Michaud HA, Hayashi G, Kuebler PJ, Hultman GK, Ariza ME, Williams MV, Batista MD, Nixon DF, Foerster J, Bowcock AM, Liao W. Protective effect of human endogenous retrovirus K dUTPase variants on psoriasis susceptibility. J Invest Dermatol. 2012; 132:1833–1840. [PubMed: 22437317]
35. Berglund LJ, Avery DT, Ma CS, Moens L, Deenick EK, Bustamante J, Boisson-Dupuis S, Wong M, Adelstein S, Arkwright PD, Bacchetta R, Bezrodnik L, Dadi H, Roifman CM, Fulcher DA, Ziegler JB, Smart JM, Kobayashi M, Picard C, Durandy A, Cook MC, Casanova JL, Uzel G, Tangye SG. IL-21 signalling via STAT3 primes human naive B cells to respond to IL-2 to enhance their differentiation into plasmablasts. Blood. 2013; 122:3940–3950. [PubMed: 24159173]
36. Cavallo P, Cianciulli A, Mitolo V, Panaro MA. Lipopolysaccharide (LPS) of helicobacter modulates cellular DNA repair systems in intestinal cells. Clin Exp Med. 2011; 11:171–179. [PubMed: 21069418]
37. Lee J, Sayed N, Hunter A, Au KF, Wong WH, Mocarski ES, Pera RR, Yakubov E, Cooke JP. Activation of innate immunity is required for efficient nuclear reprogramming. Cell. 2012; 151:547–558. [PubMed: 23101625]
38. Ohnuki M, Tanabe K, Sutou K, Teramoto I, Sawamura Y, Narita M, Nakamura M, Tokunaga Y, Nakamura M, Watanabe A, Yamanaka S, Takahashi K. Dynamic regulation of human endogenous retroviruses mediates factor-induced reprogramming and differentiation potential. Proc Natl Acad Sci U S A. 2014; 111:12426–12431. [PubMed: 25097266]
39. Steiner MK, Syrkina OL, Kolliputi N, Mark EJ, Hales CA, Waxman AB. Interleukin-6 overexpression induces pulmonary hypertension. Circ Res. 2009; 104:236–244. 228p–244. [PubMed: 19074475]
40. Kowalczyk MJ, Danczak-Pazdrowska A, Szramka-Pawlak B, Zaba R, Silny W, Osmola-Mankowska A. Expression of selected human endogenous retroviral sequences in skin and peripheral blood mononuclear cells in morphea. Arch Med Sci. 2012; 8:819–825. [PubMed: 23185190]
41. Bhardwaj N, Maldarelli F, Mellors J, Coffin JM. HIV-1 infection leads to increased transcription of human endogenous retrovirus HERV-K (HML-2) proviruses in vivo but not to increased virion production. J Virol. 2014; 88:11108–11120. [PubMed: 25056891]

42. Okahara G, Matsubara S, Oda T, Sugimoto J, Jinno Y, Kanaya F. Expression analyses of human endogenous retroviruses (HERVs): Tissue-specific and developmental stage-dependent expression of HERVs. Genomics. 2004; 84:982–990. [PubMed: 15533715]
43. Wu Y, Qi X, Gong L, Xing G, Chen M, Miao L, Yao J, Suzuki T, Furihata C, Luan Y, Ren J. Identification of BC005512 as a DNA damage responsive murine endogenous retrovirus of GLN family involved in cell growth regulation. PLoS One. 2012; 7:e35010. [PubMed: 22514700]
44. Aldred MA, Comhair SA, Varella-Garcia M, Asosingh K, Xu W, Noon GP, Thistlethwaite PA, Tuder RM, Erzurum SC, Geraci MW, Coldren CD. Somatic chromosome abnormalities in the lungs of patients with pulmonary arterial hypertension. Am J Respir Crit Care Med. 2010; 182:1153–1160. [PubMed: 20581168]
45. Li M, Vattulainen S, Aho J, Orcholski M, Rojas V, Yuan K, Helenius M, Taimen P, Myllykangas S, De Jesus Perez V, Koskenvuo JW, Alastalo TP. Loss of bone morphogenetic protein receptor 2 is associated with abnormal DNA repair in pulmonary arterial hypertension. Am J Respir Cell Mol Biol. 2014; 50:1118–1128. [PubMed: 24433082]
46. Collins PL, Kyle KE, Egawa T, Shinkai Y, Oltz EM. The histone methyltransferase SETDB1 represses endogenous and exogenous retroviruses in B lymphocytes. Proc Natl Acad Sci U S A. 2015; 112:8367–8372. [PubMed: 26100872]
47. Hanke K, Hohn O, Liedgens L, Fiddeke K, Wamara J, Kurth R, Bannert N. Staufen-1 interacts with the human endogenous retrovirus family HERV-K(HML-2) Rec and Gag proteins and increases virion production. J Virol. 2013; 87:11019–11030. [PubMed: 23926355]
48. Eyries M, Montani D, Girerd B, Perret C, Leroy A, Lonjou C, Chelghoum N, Coulet F, Bonnet D, Dorfmuller P, Fadel E, Sitbon O, Simonneau G, Tregouet DA, Humbert M, Soubrier F. EIF2AK4 mutations cause pulmonary veno-occlusive disease, a recessive form of pulmonary hypertension. Nat Genet. 2014; 46:65–69. [PubMed: 24292273]
49. Bauer EM, Zheng H, Comhair S, Erzurum S, Billiar TR, Bauer PM. Complement C3 deficiency attenuates chronic hypoxia-induced pulmonary hypertension in mice. PLoS One. 2011; 6:e28578. [PubMed: 22194859]
50. Garcia-Etxebarria K, Jugo BM. Genome-wide reexamination of endogenous retroviruses in Rattus norvegicus. Virology. 2016; 494:119–128. [PubMed: 27107945]

Clinical Perspectives

What is new

- SAM domain and HD1 domain-containing protein (SAMHD1) is an innate immune factor that suppresses HIV replication. We identified SAMHD1 immune complexes in lungs from pulmonary arterial hypertension (PAH) patients.
- Elevated SAMHD1 led to the discovery that human endogenous retrovirus (HERV-K) gene products, HERV-K envelope and dUTPase, were elevated in PAH lungs.
- The heightened expression of HERV-K dUTPase was observed in PAH circulating monocytes and induced pluripotent stem cells (iPSC).
- Treatment with HERV-K dUTPase induced SAMHD1 and cytokines, including IL6, in circulating monocytes as well as PAEC, and promoted apoptosis in PAEC.
- Rats treated with HERV-K dUTPase developed pulmonary hypertension.

What are the clinical implications

- Current treatments for PAH improve survival but are not disease modifying because they do not address pathological mechanisms of inflammation and immune dysregulation.
- We show that perivascular immune complexes containing the antiviral protein SAMHD1 result from elevation in products of the endogenous retrovirus HERV-K that are expressed in PAH perivascular macrophages and circulating monocytes.
- The HERV-K dUTPase activates B cells, elevates cytokines in monocytes and PAEC and increases PA vulnerability to apoptosis, thus contributing to sustained inflammation, immune dysregulation and progressive obliterative vascular remodeling.
- Harnessing mechanisms that repress HERV-K expression and sequelae could prevent and reverse PAH.

A

Gene	PAH	PAH	PAH	CON	CON	CON
Tubulin beta chain	23	21	19	1	3	0
Clathrin heavy chain 1	8	11	8	0	0	0
Spectrin beta chain, brain 1	18	10	13	0	0	1
40S ribosomal protein S20	6	5	4	0	0	0
F-actin-capping protein subunit alpha-1	5	6	4	0	0	0
Myosin-Ib	21	17	8	0	0	0
Alpha-actinin-4	31	19	12	3	0	0
Actin-related protein 3	10	6	5	0	0	0
Myosin-11	276	166	85	32	8	0
Tropomodulin-3	23	13	8	0	0	0
Myosin-Id	31	8	21	0	0	0
Desmocollin-1	7	11	4	0	0	0
Actin-related protein 2	16	8	6	0	0	0
Eukaryotic translation initiation factor 2 subunit 3	4	11	7	1	0	0
rRNA 2"-O-methyltransferase fibrillarin	3	7	4	0	0	0
Actin, cytoplasmic 2	14	9	5	2	1	1
Myosin-Ic	56	34	12	2	3	2
Protein-glutamine gamma-glutamyltransferase 2	4	9	10	0	0	3
SAM domain and HD domain-containing protein 1	6	3	7	0	2	0
Actin-related protein 2/3 complex subunit 4	3	7	4	1	0	0
Myosin-9 OS	658	344	137	103	26	4
CD59 glycoprotein	3	5	2	0	0	0
40S ribosomal protein S13	7	9	9	1	6	4
40S ribosomal protein S3a	5	17	18	6	2	1
Gelsolin	47	25	10	12	2	1
ATP synthase subunit alpha, mitochondrial	14	12	16	12	8	9
Actin, cytoplasmic 1	143	153	80	115	38	31
Actin, aortic smooth muscle	17	3	10	0	3	1
Myosin light polypeptide 6	16	10	1	0	0	0

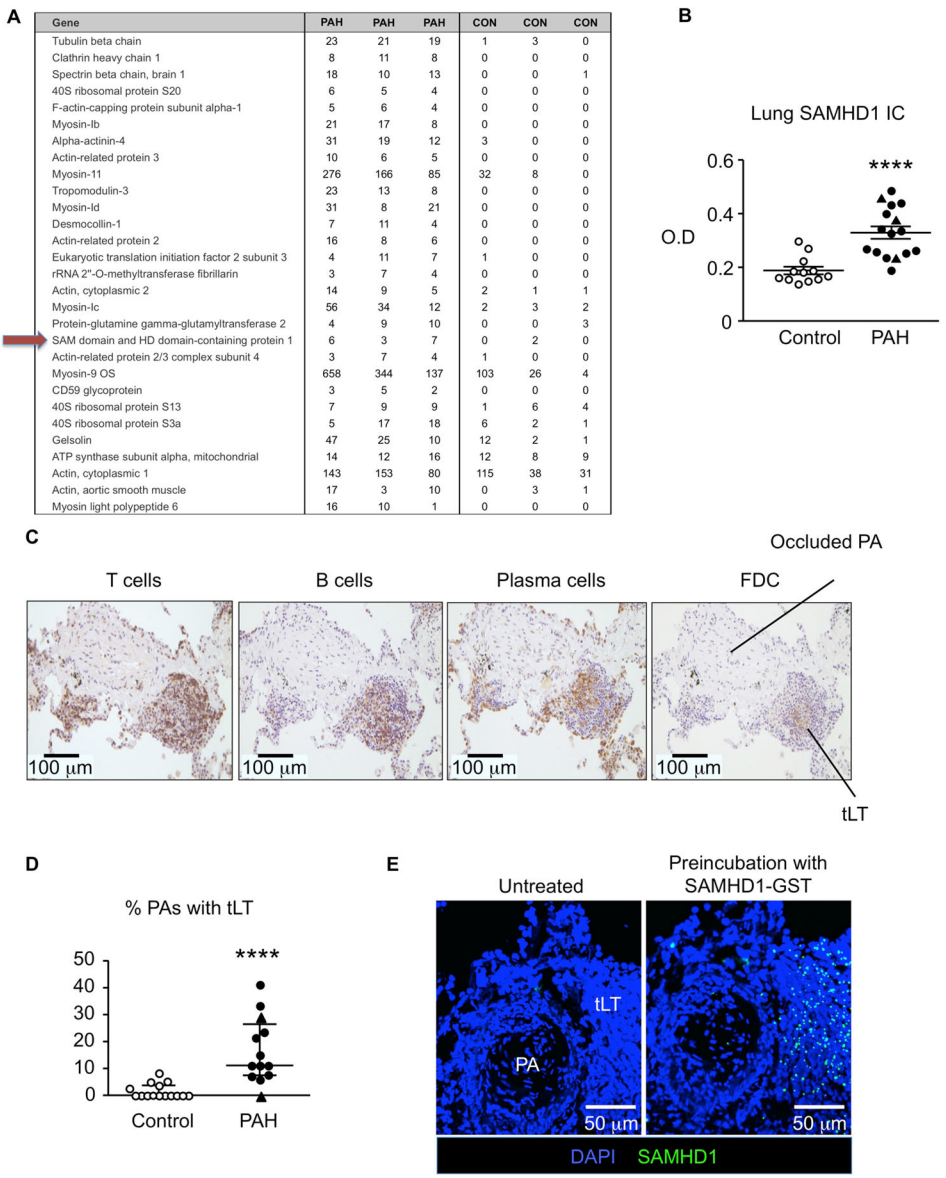

Figure 1. SAMHD1 a target antigen in immune complexes in PAH lungs

(A) C1q immunoprecipitation followed by liquid chromatography tandem mass spectrometry identified target antigens of immune complexes in PAH (n=3) and control (n=3) lungs. Targets are ranked by q value according to the SAM statistic and all were within the false discovery rate (FDR) of 5%. **(B)** SAMHD1 immune complexes measured by ELISA in PAH (n=16) and control (n=12) lungs. ****P<0.0001 by Welch test. **(C)** Representative sections from a PAH lung show tertiary lymphoid tissue (tLT), characterized by positive immunoreactivity to markers of T cells (CD3), B cells (CD19), plasma cells (rough endoplasmic reticulum-associated protein p63) and follicular dendritic cells (FDC; 120 kDa FDC protein). **(D)** Number of PAs with associated tertiary lymphoid tissue relative to total PAs was calculated as a percentage from lung tissue sections in each control (n=15) and each PAH patient (n=13) and controls. ****P<0.0001 by Mann-Whitney test. **(E)**

SAMHD1 immunoreactive foci in tertiary lymphoid tissue detected by applying recombinant GST-tagged SAMHD1 protein to lung tissue sections, followed by an anti-GST-FITC conjugated antibody Negative controls were treated with PBS, followed by anti-GST-FITC conjugated antibody. Nuclei were stained by DAPI (blue). Ranges represent mean ± SEM (B) and median with interquartile range (D). Closed symbols (PAH), open symbols (controls), closed triangles hereditary PAH (HPAH).

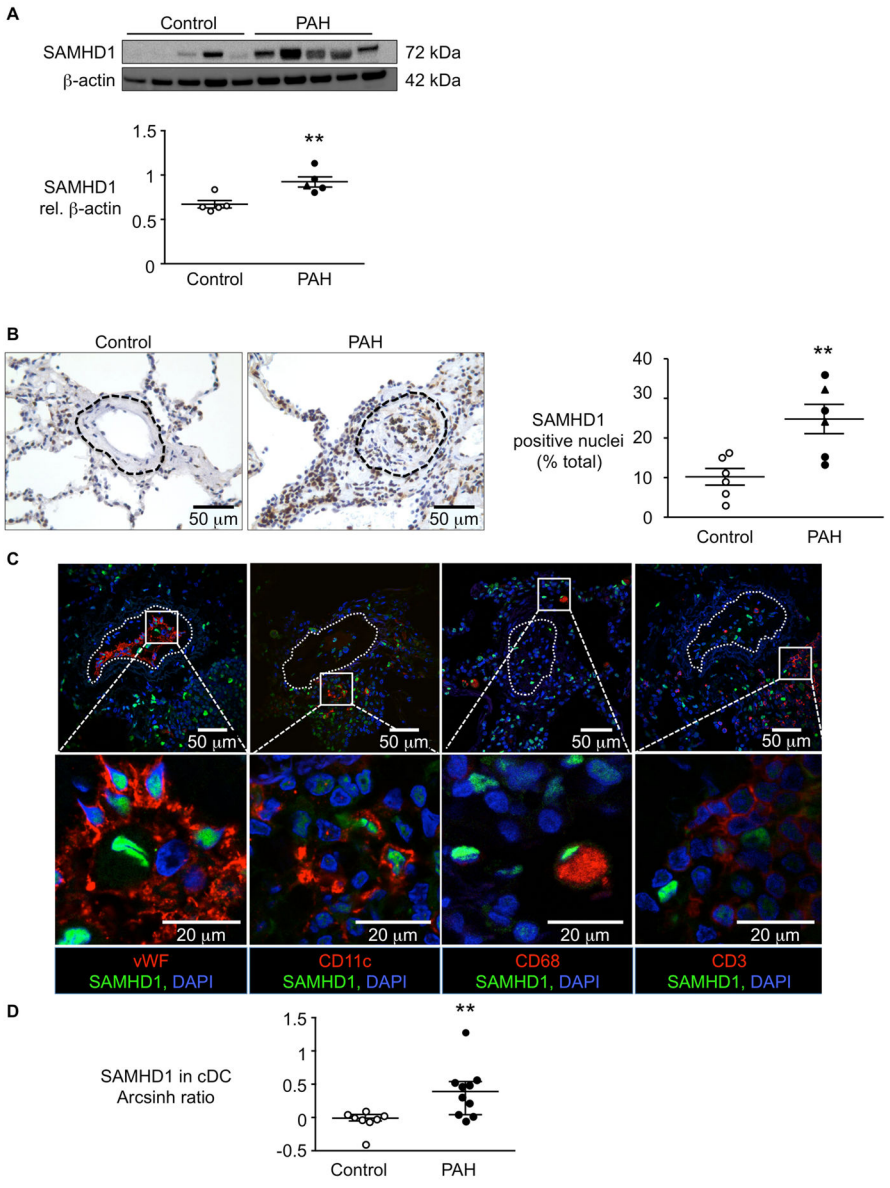

Figure 2. Elevated SAMHD1 in PAH lung cells and in circulating classical dendritic cells (cDC)

(A) Representative western immunoblot with densitometric quantitation of SAMHD1 in lung lysates assessed in PAH (n=5) vs. control (n=5) lungs. **P<0.01 by Student's t-test. **(B)** Representative immunohistochemistry of SAMHD1 in pulmonary artery (PA) from a donor (control) lung, and from a PA of similar size and at similar airway level from a lung of a PAH patient. Below, percent nuclei that stained for SAMHD1 in all arteries in a lung section in PAH (n=6) vs. control (n=6) lungs, calculated using the ImmunoRatio program. The dashed line indicates the vessel boundary including the adventitia, within which % SAMHD1 positive cells was calculated. **P<0.01 by Student's t-test. **(C)** Confocal microscopic images of sections immunolabeled with SAMHD1 (green), and four lineage markers (red): left to right, vWF (endothelial cells), CD11c (dendritic cells), CD68 (macrophages) and CD3 (T cells). Nuclei were stained with DAPI (blue). Dashed line

indicates vessel boundary. **(D)** SAMHD1 assessed by CyTOF in circulating classical dendritic cells (cDCs) from PAH patients (n=10) or controls (n=8). Data are shown as the calculated difference of inverse hyperbolic sine medians between control and PAH samples (Arcsinh Ratio). **P<0.01 by Mann-Whitney test. Ranges represent mean ± SEM (A, B) and median with interquartile range (D). Closed symbols (PAH), open symbols (controls), closed triangles hereditary PAH (HPAH).

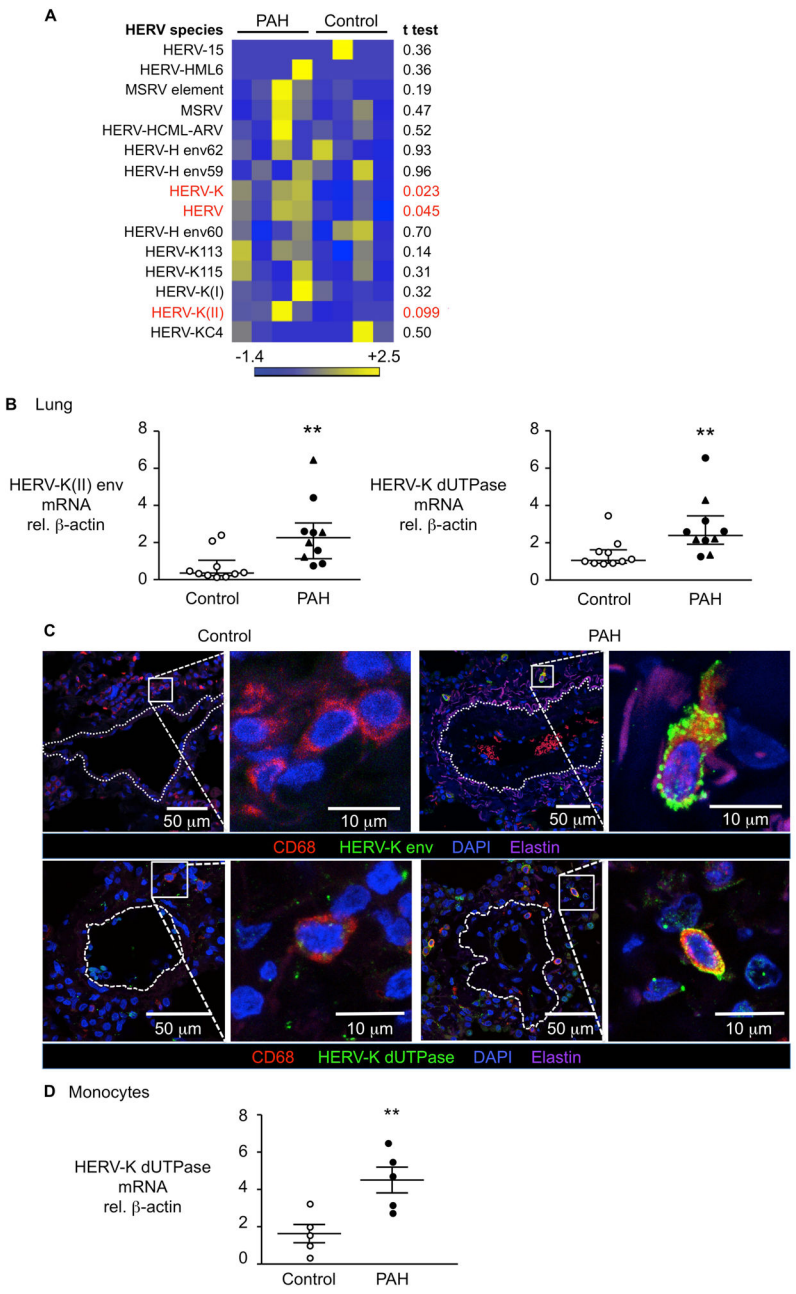

Figure 3. Elevated HERV-K and HERV-K dUTPase detected in lungs and circulating monocytes from PAH vs. controls

(A) HERV species in lung tissue from PAH patients (n=4) and controls (n=4) by metagenomic sequencing described in Methods. MSRV, multiple sclerosis-associated retrovirus. **(B)** HERV-K(II) envelope and dUTPase mRNA by qPCR in lung extracts from PAH patients (n=10) and controls (n=10). **P<0.01 by Mann-Whitney test. **(C)** Confocal microscopy images of representative lung sections from a PAH patient and a control, show cells immunolabeled for HERV-K envelope protein or HERV-K dUTPase (green), macrophages ($CD68^+$, red) and nuclei (DAPI, blue). Dashed line indicates vessel boundary. Elastin auto-fluorescence appears pink. (D) HERV-K dUTPase mRNA in circulating

monocytes from PAH patients (n=5) vs. controls (n=5). **P<0.01 by Student's t-test. Ranges represent mean ± SEM (D) and median with interquartile range (B). Closed symbols are PAH patients, open symbols are controls, closed triangles represent hereditary PAH (HPAH) patients.

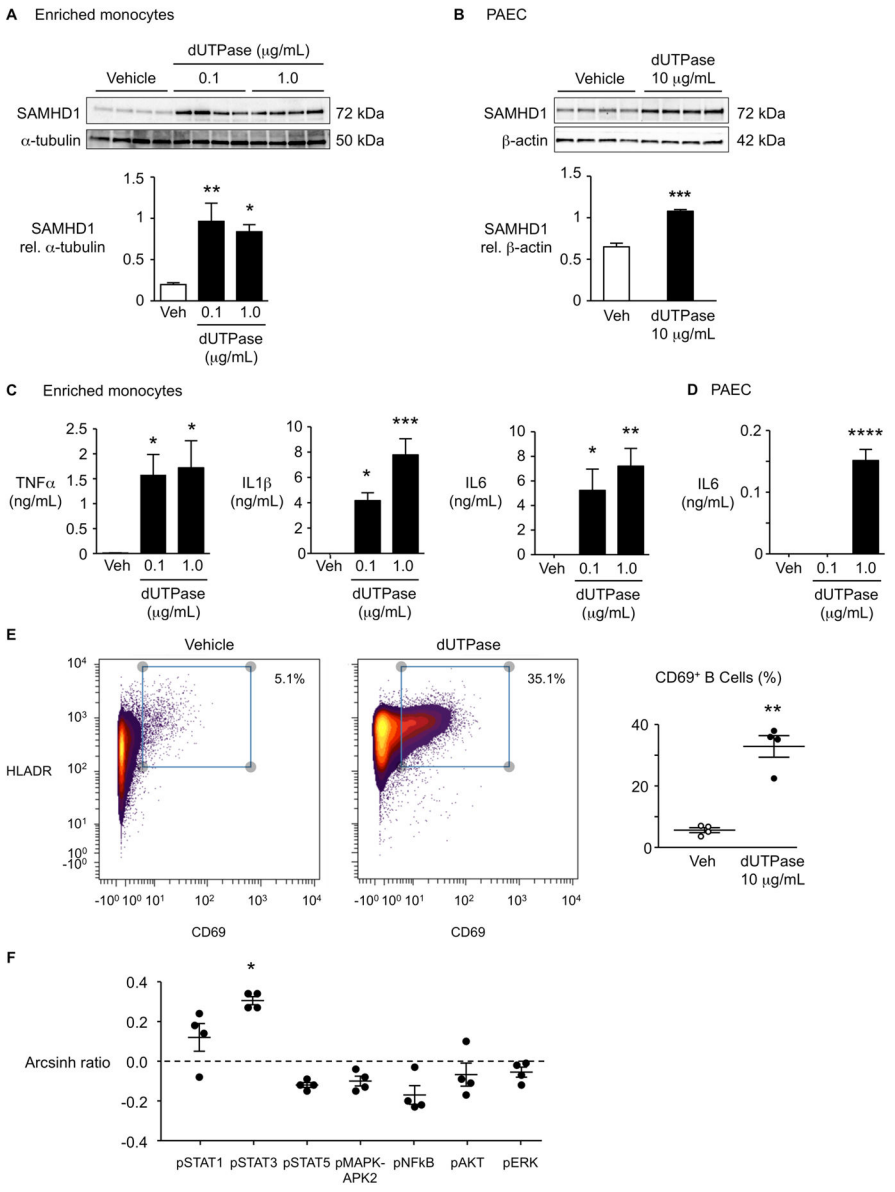

Figure 4. HERV-K dUTPase increases SAMHD1, cytokines in enriched monocytes and pulmonary arterial endothelial cells (PAEC), and activates B cells

(A, B) Enriched monocytes from PBMC **(A)** or PAEC **(B)** from healthy donors were treated with recombinant HERV-K dUTPase (0.1, 1 or 10 μg/mL) for 24 hr, and SAMHD1 was assessed by western immunoblot. **(C, D)** TNFα, IL1β and IL6 measured by ELISA in medium of enriched monocytes **(C)** or PAEC **(D),** treated with 0.1 or 1 μg/mL HERV-K dUTPase. **(E)** $CD69^{+}$ B cells**,** and **(F)** signaling molecules assessed by CyTOF following HERV-K dUTPase (10 μg/mL for 24 hr). Signal induction was calculated as the difference of inverse hyperbolic sine medians between untreated (Control, Con) and HERV-K dUTPase-treated samples (arcshinh ratio). Ranges represent mean ± SEM of n=4 different experiments. *P<0.05, **P<0.01, ***P<0.001, ****P<0.0001 by Student's t-test (B, E), or

by one-way ANOVA and post hoc Dunnett's test (A, C and D). In (F), Bonferroni-adjusted P-value ($P=7.14X10^{-3}$) is applied to response with arcsinh ratio > |0.2|).

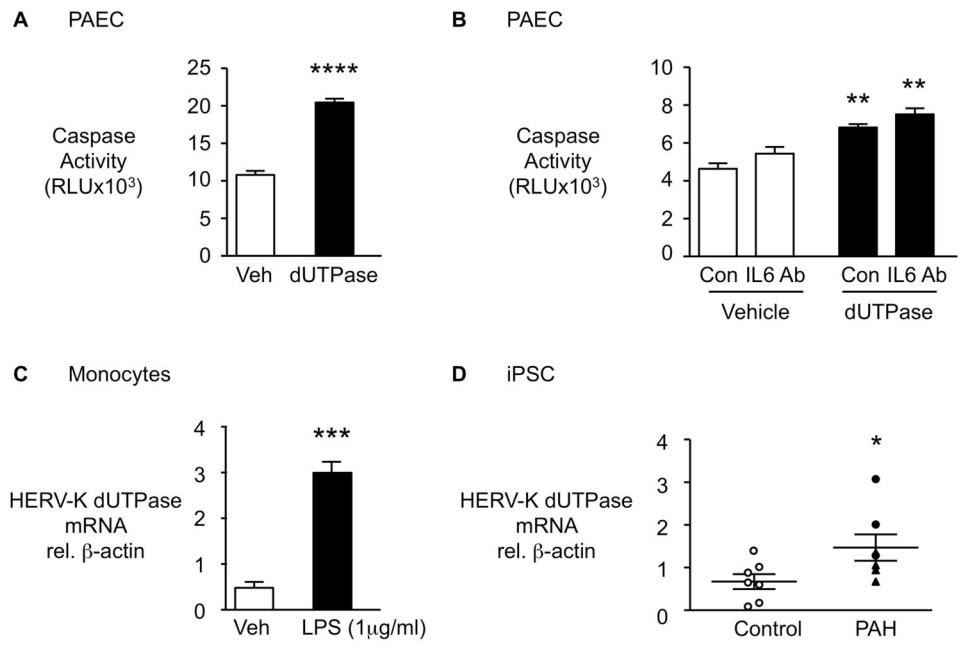

Figure 5. HERV-K dUTPase increases apoptosis in pulmonary arterial endothelial cells (PAEC) in an IL6 independent manner, is induced in monocytes by LPS and is elevated in iPSC from PAH patients vs. controls

(A) PAEC were treated with 10 μg/mL HERV-K dUTPase and apoptosis was assessed by Caspase-Glo 3/7 assay following overnight serum withdrawal (n=4). (B) PAEC were pre-treated with neutralizing IL6 antibody (IL6 Ab) or isotype control (Con) before HERV-K dUTPase treatment (n=4). (C) HERV-K dUTPase mRNA by qPCR in monocytes stimulated with LPS 1μg/ml (n=3). (D) HERV-K dUTPase mRNA by qPCR in iPSC from PAH patients (n=7) and controls (n=7). Ranges represent mean ± SEM. *P<0.05, ***P<0.001, ****P<0.0001 by Student's t-test (A, C, D). In (B), **P<0.01, HERV-K dUTPase vs. Vehicle treatment, by one-way ANOVA and post hoc Tukey test. Closed symbols (PAH), open symbols (controls), closed triangles hereditary PAH (HPAH).

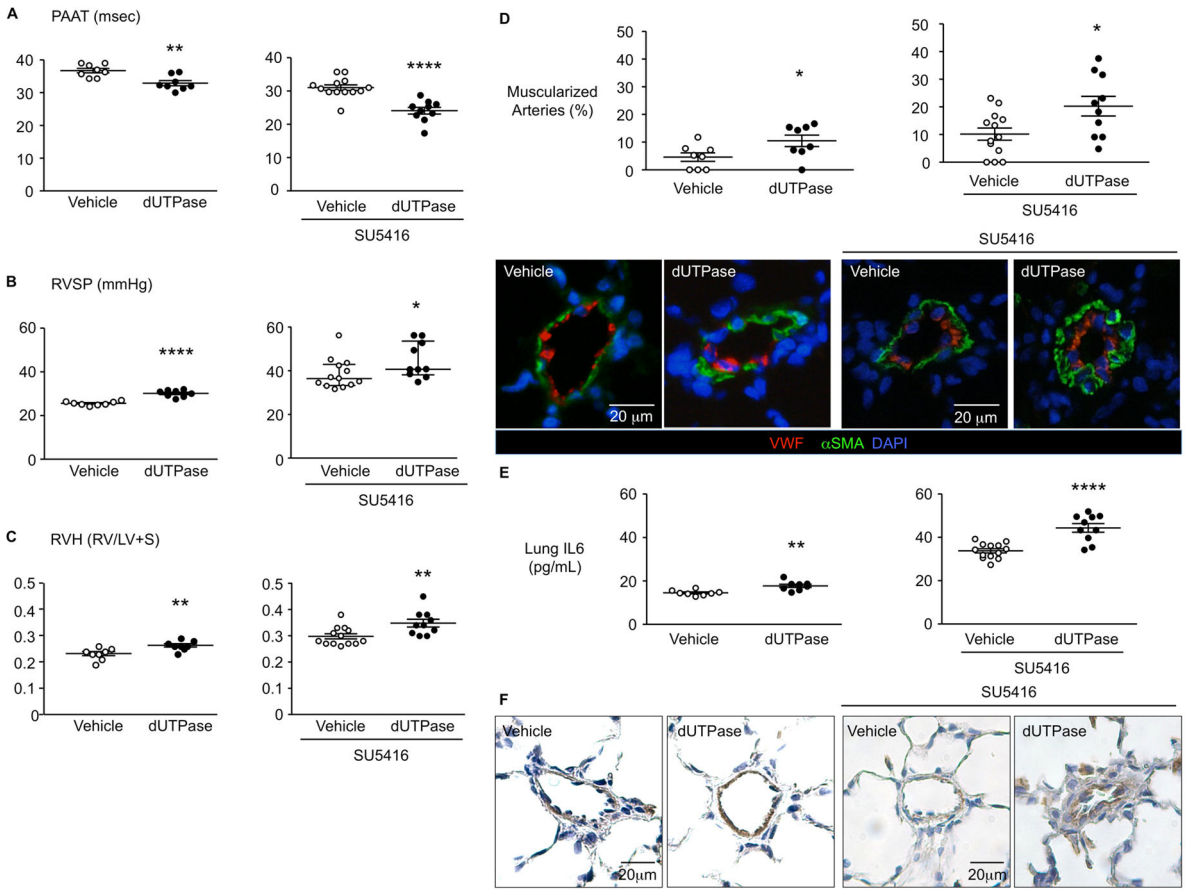

Figure 6. HERV-K dUTPase causes pulmonary hypertension in a rat

Adult male Sprague Dawley rats (7 wks, 180–200 g) were treated with HERV-K dUTPase (0.2 mg/kg), or saline (vehicle) once a week, for three weeks (LHS) or were pre-treated with the VEGF receptor 2 blocker SU5416 (20 mg/kg) (RHS). Pulmonary and cardiac functions were evaluated on day 21. **(A)** Pulmonary artery acceleration time (PAAT). **(B)** Right ventricular systolic blood pressure (RVSP). **(C)** Right ventricular hypertrophy (RVH). **(D)** Confocal microscopic images of lung sections of treated and control rats, immunolabeled for αSMA (green, smooth muscle cell marker), and vWF (red, endothelial cells) on the left, with the % of muscularized distal vessels on the right. **(E, F)** IL6 levels in lungs, by ELISA (E) and IL6 staining by IHC (F). Saline (n=8) or HERV-K dUTPase (n=8), SU5416 + Saline (n=13) or SU5416 + HERV-K dUTPase (n=10). Ranges represent mean ± SEM (A, C, D, E and B, left) and median with interquartile range (B, right). *P<0.05 **P<0.01 and ****P<0.0001 by Student's t-test in (A, C, D and E) or by Mann Whitney test (B).

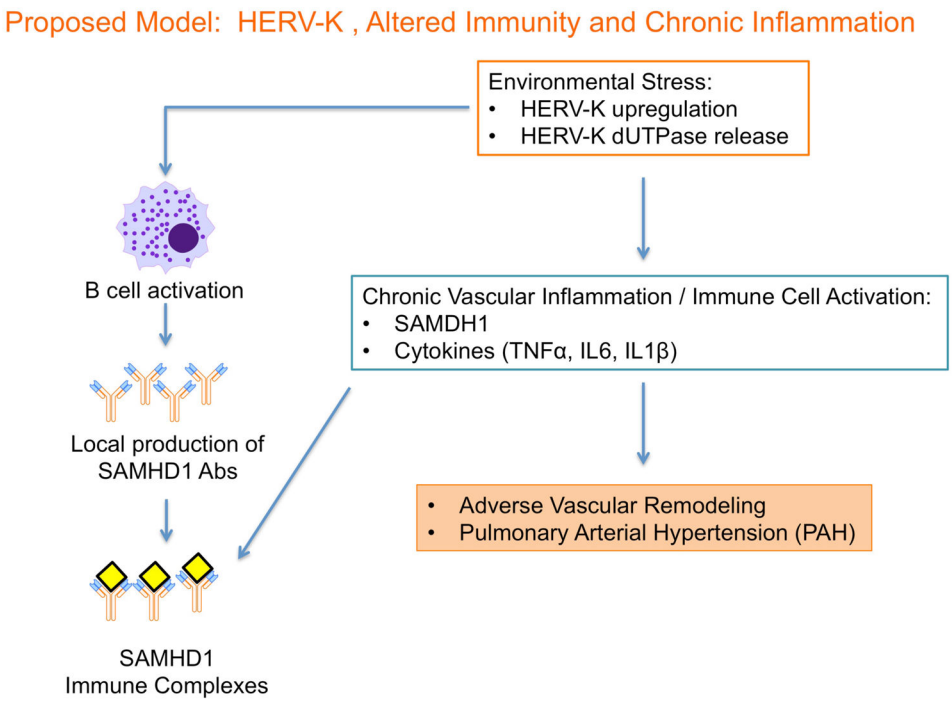

Figure 7. Proposed model for the role of HERV-K and SAMHD1 in PAH

The endogenous retrovirus HERV-K is expanded, possibly as a result of an environmental or genotoxic stress. The product, HERV-K dUTPase, and the subsequent activation of vascular, inflammatory and immune cells lead to adverse vascular remodeling and PAH.